Novel Tetranuclear Orthometalated Complexes of Pd(II) and Pt(II) Derived from *p*-Isopropylbenzaldehyde Thiosemicarbazone with Cytotoxic Activity in *cis*-DDP Resistant Tumor Cell Lines. Interaction of These Complexes with DNA

Adoración G. Quiroga,[†] José M. Pérez,[†] Isabel López-Solera,[†] José R. Masaguer,[†,‡] Antonio Luque,[§] Pascual Román,[§] Andy Edwards,[∥] Carlos Alonso,[⊥] and Carmen Navarro-Ranninger*[,†]

Departamento de Química Inorgánica, Facultad de Ciencias, Universidad Autónoma de Madrid, 28049 Madrid, Spain, Departamento de Química Inorgánica, Facultad de Ciencias, Universidad del País Vasco, 48080 Bilbao, Spain, Department of Chemistry, University of Newcastle, U.K., Centro de Biología Molecular "Severo Ochoa", CSIC-Universidad Autónoma de Madrid, 28049 Madrid, Spain

Received August 4, 1997

The reaction of *p*-isopropylbenzaldehyde thiosemicarbazone [p-is.TSCN], **1**, with palladium(II) acetate and potassium tetrachloroplatinate yielded two tetrameric orthopalladated isomers, $[Pd(p\text{-is.TSCN})]_4$ (complexes **2** and **3**), and the platinum analogue $[Pt(p\text{-is.TSCN})]_4$ (complex **4**), respectively. All of these complexes contain the thiosemicarbazone bonded as a terdentate ligand to the metallic atom, through the thiol sulfur, the azomethinic nitrogen and the ortho carbon of the *p*-isopropylphenyl ring to which the imine group is attached to as deduced from the study of the IR, NMR, and XRD spectra of complexes **2** and **4**. Complexes **2** and **4** crystallize in the centrosymmetric monoclinic space group *C*2/*c*, with $Z = 8$. Unit cell parameters for complex **2** are as follows: $a = 25.742(5)$ Å, $b = 19.560(4)$ Å, $c = 24.199(5)$ Å, $\beta = 101.70(3)^o$. Unit cell parameters for complex **4** are as follows: $a = 25.8728(19)$ Å, $b = 19.5053(14)$ Å, $c = 24.0899(16)$ Å, $\beta = 101.305(2)^o$. As can be deduced from the NMR study, the palladated isomers **2** and **3** interconvert in DMSO which may be a consequence of the existence in both complexes of a flexible eight-membered ring with alternating Pd−S atoms. The testing of the cytotoxic activity of these compounds against several human and murine cell lines sensitive and resistant to cisplatin (*cis*-DDP) suggests that compounds **2**, **3,** and **4** may be endowed with important anticancer properties since they elicit IC_{50} values in the μM range as does the clinically used drug *cis*-DDP, and, moreover, they display cytotoxic activity in tumor lines resistant to *cis*-DDP. The analysis of the interaction of these novel tetrameric cyclometalated compounds with DNA suggests that they form DNA interhelical cross-links.

Introduction

Thiosemicarbazones, such as *p*-isopropylbenzaldehyde and 2-acetylpyridin thiosemicarbazone and derivative complexes, have considerable pharmacological interest due to their antibacterial, antiviral, and antitumor activities.[1] The antitumor activity of them seems to be due to an inhibition of DNA synthesis produced by the modification in the reductive conversion of ribonucleotides to deoxyribonucleotides. This activity is enhanced by the presence of some metallic ions due to their ability to form chelates.[2]

Thiosemicarbazones usually react as chelating ligands with transition metal ions by bonding through the sulfur and the azomethinic nitrogen atoms, although in some cases they behave as terdentate ligands and bond through the sulfur and two nitrogen atoms.[3] There are many studies involving thiosemicarbazones with different metal atoms, but only a few papers with palladium as metal[4] and, as far as we know, none with complexes having Pd−C bonds.

Our interest in the cyclometalation process[5] and the fact that cyclometalated complexes may have potential antitumor activity[6] led us to prepare complexes of palladium(II) and platinum(II) with *p*-isopropylbenzaldehyde thiosemicarbazone (p-is.TSCN) as a first step in studying whether metallic complexes of palladium and platinum coupled with the p-is.TSCN ligand may enhance the pharmacological activity of the ligand and whether different isomers display different cytotoxic activity. In the present paper, we report the synthesis and characterization of novel tetranuclear $[Pd(p\text{-is.TSCN})]_4$ isomers, **2** and **3**, to compare their pharmacological activity with that of their platinum analogue $[Pt(p\text{-is.TSCN})]_4$, **4**. The data obtained from the cytotoxicity testing of these complexes against human and murine tumor cell lines sensitive or resistant to *cis*-DDP (Jurkat, Pam-Ras), normal murine keratinocites (Pam), and two *cis*-DDP resistant primary cultures of glioma cells, derived from byopsies of death cancer patients, clearly indicate that complexes **2**, **3**, and **4** may be considered potential antitumor agents since they exhibit IC_{50} values in the μM range as *cis*-DDP and, moreover, they show important cytotoxic activity against cells resistant to this clinically used drug. On the other hand, the analysis of the interaction of complexes **2**, **3**, and **4** with DNA indicates that they form interhelical cross-links, a unique feature that is not shown by *cis*-

* To whom correspondence should be sent.
[†] Universidad Autónoma de Madrid.
[‡] Deceased June 19, 1997.
[§] Universidad del País Vasco.
[∥] University of Newcastle.
[⊥] CSIC-Universidad Autónona de Madrid.

S0022-2623(97)00520-7 CCC: $15.00
Published on Web 03/28/1998

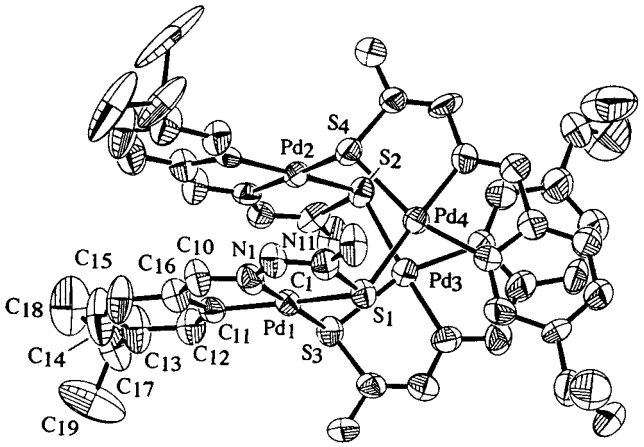

Figure 1. Molecular structure of complex **2** showing the atom numbering scheme for the eight-membered ring and one compound **1** unit. The other compound **1** units are similar, changing the first digit, which indicates the corresponding palladium atom to which they are attached to. H atoms have been omitted for clarity.

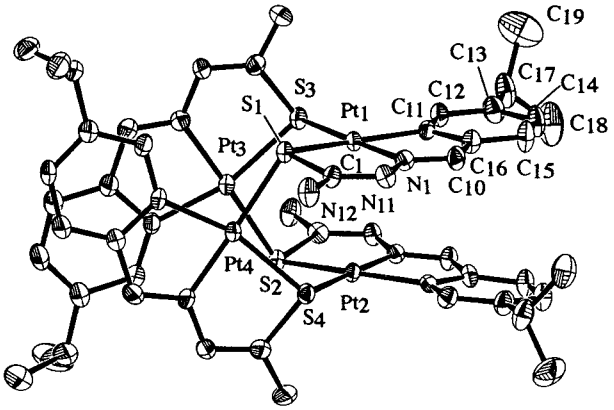

Figure 2. Molecular structure of complex **4** showing the atom numbering scheme for the eight-membered ring and one compound **1** unit. The other compound **1** units are similar, changing the first digit, which indicates the corresponding palladium atom to which they are attached to. H atoms have been omitted for clarity.

DDP and that may be in part responsible for the biochemical mechanism of these novel tetrameric cyclometalated complexes.

Results and Discussion

Synthesis and Characterization of the Complexes. The reaction between equimolecular amounts of $Pd(AcO)_2$ and the potentially tridentate CNS donor ligand p-is.TSCN, **1**, in acetic acid at 40 °C under argon for 24 h resulted in the formation of the complexes **2** (yellow) and **3** (dark orange). These complexes were separated and purified by chromatography. Complex **2** is insoluble in most organic solvents, only slightly soluble in chloroform, and soluble in DMSO (dimethyl sulfoxide) and DMF (*N*,*N*-dimethylformamide), whereas complex **3** is soluble in most organic solvents, except in *n*-hexane, and is slightly soluble in diethyl ether.

The tetranuclear cyclometalated complex [Pt(p-is.TSCN)]$_4$, **4**, was prepared by reaction of equivalents amounts of K_2PtCl_4 with p-is.TSCN, **1**, using MeOH as solvent for 15 days at room temperature. The platinum complex, **4,** is pale orange and soluble in most organic solvents except in *n*-hexane and diethyl ether.

Complexes **2**, **3**, and **4** were characterized by elemental analysis, FAB mass spectrometry, and IR and NMR spectroscopy. The FAB mass spectra for **2**, **3**, and **4** show a peak at *m*/*z* 1303.1, 1304.1, and 1657.7, respectively, suggesting the existence of tetrameric structures for all the complexes. The structure of complexes **2** and **4** has been determined by X-ray diffraction (see below). NMR spectroscopy data are consistent with the solid-state structure determined by X-ray crystallography.

Crystal Structure of Complexes 2 and 4. The palladium complex **2**, crystallizes with acetic acid as solvation molecules and the platinum complex **4**, with molecules of dichloromethane and methanol. A perspective view of the tetrameric [Pd(p-is.TSCN)]$_4$ entity with the atomic numbering scheme is depicted in Figure 1, and the perspective view corresponding to the platinum complex **4** is shown in Figure 2. Selected bond distances and angles are summarized in Tables 1 and 2, respectively.

In both cases the structure consists of a tetramer. The core of **2** and **4** consists of an eight-membered ring of alternating M (Pd (II) in **2**, Pt(II) in **4**) and S atoms in a boat conformation. The geometry around the metallic atom is approximately square-planar. The remaining two sites of each square-planar M (Pd (II) in **2**, Pt(II) in **4**) coordination sphere are occupied by the iminic nitrogen and the ortho carbon of the *p*-isopropylphenyl ring to which the imine group is attached to. The two five-member chelate rings involving the metallic atom are almost coplanar. The Pd−Pd distances (Pd(1)−Pd(2) = 3.341(3) Å and Pd(3)−Pd(4) = 3.330(2) Å) and the Pt−Pt distances (Pt(1)−Pt(2) = 3.3218(4) Å and Pt(3)−Pt(4)= 3.3205(4) Å) indicate no direct bond between the metallic atoms, but a very weak interaction can be postulated in agreement with the reported values for polynuclear complexes with Pd or Pt, a Pd_4 core (2.549(2)−3.539(1) Å) and 2.537(1)-3.507(1) Å platinum complexes.[7] A similar ring disposition has been described in palladium complexes with amido[8] and in palladium and platinum complexes with 2-(1-naphthyl)-benzothiazoline[9] as ligands.

M−N bond distances of 1.98(2)−1.99(2) Å for **2** and 1.978(4)−1.996(5) for **4** and M−C (1.99(2) to 2.02(2) Å for **2** 2.014(5) to 2.020(5) Å) in the five-membered orthometallacycle are analogous to those found in other similar. The trans influence of the metalated carbon[10] can be reflected in the lengthening of the M−S distance trans to the carbon atom (2.364(7) to 2.389(5) Å for palladium complex **2**, and 2.3506(16) to 2.3514(14) Å for platinum complex **4**) with respect to the M−S distance trans to the imine nitrogen (2.308(6) to 2.316(5) Å for **2**, and 2.3036(15)−2.3009(16) for **4**) and within the range of the M−S distance described for other polynuclear complexes.[8,11]

The IR spectra indicating that the C=N stretching mode for the ligand **1** at 1594 cm^{-1} shifts to lower frecuencies, at 1579 cm^{-1} in **2**, at 1580 cm^{-1} in **3**, and at 1583 cm^{-1} in **4**, suggests coordination to the metallic atom through the iminic nitrogen in all complexes.[3] A new band at 1625 cm^{-1} in **2**, at 1623 cm^{-1} in **3**, and at 1611 cm^{-1} in **4** can be attributed to the ν(C=N−N=C) vibrational mode.[4a] The absence of the two bands at 829 and 820 cm^{-1} attributed to the ν(C=S) mode in the

Table 1. Selected Bond Lengths (Å) for Complexes **2** and **4**

complex **2**				complex **4**			
Pd(1)−S(1)	2.382(6)	N(2)−N(21)	1.38(2)	Pt(1)−S(1)	2.3491(16)	N(2)−N(21)	1.388(7)
Pd(1)−S(3)	2.316(5)	N(2)−C(20)	1.32(3)	Pt(1)−S(3)	2.3036(15)	N(2)−C(20)	1.292(7)
Pd(1)−N(1)	1.98(2)	C(20)−C(26)	1.41(3)	Pt(1)−N(1)	1.996(5)	C(20)−C(26)	1.451(7)
Pd(1)−C(11)	2.01(2)	C(21)−C(26)	1.44(3)	Pt(1)−C(11)	2.020(5)	C(21)−C(16)	1.425(7)
Pd(2)−S(2)	2.389(5)	N(22)−C(2)	1.32(3)	Pt(2)−S(2)	2.3514(14)	N(22)−C(26)	1.355(8)
Pd(2)−S(4)	2.308(6)	S(3)−C(3)	1.79(2)	Pt(2)−S(4)	2.2958(16)	S(3)−C(3)	1.789(6)
Pd(2)−N(2)	1.98(2)	N(31)−C(3)	1.27(3)	Pt(2)−N(2)	1.994(5)	N(31)−C(3)	1.306(8)
Pd(2)−C(21)	2.00(2)	N(3)−N(31)	1.40(3)	Pt(2)−C(21)	2.015(5)	N(3)−N(31)	1.385(7)
Pd(3)−S(2)	2.306(6)	N(3)−C(30)	1.27(3)	Pt(3)−S(2)	2.2924(16)	N(3)−C(30)	1.288(9)
Pd(3)−S(3)	2.378(6)	C(30)−C(36)	1.46(4)	Pt(3)−S(3)	2.3506(16)	C(30)−C(36)	1.443 (9)
Pd(3)−N(3)	1.98(2)	C(31)−C(36)	1.41(4)	Pt(3)−N(3)	1.985(4)	C(31)−C(36)	1.435(9)
Pd(3)−C(31)	2.02(2)	N(32)−C(3)	1.38(3)	Pt(3)−C(31)	2.014(5)	N(32)−C(3)	1.362(8)
Pd(4)−S(1)	2.309(6)	S(4)−C(4)	1.77(2)	Pt(4)−S(1)	2.3009(16)	S(4)−C(4)	1.798(6)
Pd(4)−S(4)	2.364(7)	N(4)−N(41)	1.41(3)	Pt(4)−S(4)	2.3475(15)	N(41)−C(4)	1.312(8)
Pd(4)−N(4)	1.99(2)	N(4)−C(40)	1.25(3)	Pt(4)−N(4)	1.978(4)	N(4)−N(41)	1.376(7)
Pd(4)−C(41)	1.99(2)	N(41)−C(4)	1.29(3)	Pt(4)−C(41)	2.015(5)	N(4)−C(40)	1.303(9)
S(1)−C(1)	1.78(2)	C(40)−C(46)	1.47(4)	S(1)−C(1)	1.798(5)	C(40)−C(46)	1.433(9)
N(11)−C(1)	1.30(3)	C(41)−C(46)	1.42(4)	N(11)−C(1)	1.296(7)	C(41)−C(46)	1.412(9)
N(1)−N(11)	1.39(2)	N(42)−C(4)	1.33(3)	N(1)−N(11)	1.394(7)	N(42)−C(4)	1.349(8)
N(1)−C(10)	1.32(3)	Pd(1)−Pd(2)	3.341(3)	N(1)−C(10)	1.284(7)	Pt(1)−Pt(2)	3.3218(4)
C(10)−C(16)	1.47(3)	Pd(3)−Pd(4)	3.330(2)	C(10)−C(16)	1.430(8)	Pt(3)−Pt(4)	3.3205(4)
C(11)−C(16)	1.35(3)	Pd(1)−Pd(3)	3.773(2)	C(11)−C(16)	1.411(9)	Pt(1)−Pt(3)	3.7074(4)
N(12)−C(1)	1.36(3)	Pd(1)−Pd(4)	3.841(3)	N(12)−C(1)	1.350(7)	Pt(1)−Pt(4)	3.8581(5)
S(2)−C(2)	1.77(2)	Pd(2)−Pd(4)	3.743(3)	S(2)−C(2)	1.798(6)	Pt(2)−Pt(4)	3.8472(5)
N(21)−C(2)	1.33(3)	Pd(2)−Pd(3)	3.769(2)	N(21)−C(2)	1.312(8)	Pt(2)−Pt(3)	3.7784(4)

Table 2. Selected Bond Angles (deg) for Complexes **2** and **4**

complex **2**				complex **4**			
S(1)−Pd(1)−S(3)	100.3(2)	Pd(4)−S(1)−C(1)	101.9(8)	S(1)−Pt(1)−S(3)	99.02(5)	Pt(4)−S(1)−C(1)	99.77(19)
S(1)−Pd(1)−N(1)	81.4(5)	Pd(2)−S(2)−Pd(3)	106.8(2)	S(1)−Pt(1)−N(1)	83.57(15)	Pt(2)−S(2)−Pt(3)	108.90(6)
S(3)−Pd(1)−C(11)	97.8(6)	Pd(2)−S(2)−C(2)	93.9(7)	S(3)−Pt(1)−C(11)	96.61(14)	Pt(2)−S(2)−C(2)	93.9(2)
N(1)−Pd(1)−C(11)	80.4(8)	Pd(3)−S(2)−C(2)	101.1(8)	N(1)−Pt(1)−C(11)	80.8(2)	Pt(3)−S(2)−FC(2)	102.7(2)
S(2)−Pd(2)−S(4)	102.5(2)	Pd(1)−S(3)−Pd(3)	107.0(2)	S(2)−Pt(2)−S(4)	99.56(5)	Pt(1)−S(3)−Pt(3)	105.61(6)
S(2)−Pd(2)−N(2)	82.1(5)	Pd(1)−S(3)−C(3)	102.3(7)	S(2)−Pt(2)−N(2)	83.06(13)	Pt(1)−S(3)−C(3)	102.06(19)
S(4)−Pd(2)−C(21)	93.3(6)	Pd(3)−S(3)−C(3)	92.7(8)	S(4)−Pt(2)−C(21)	95.95(15)	Pt(3)−S(3)−C(3)	93.3(2)
N(2)−Pd(2)−C(21)	82.3(8)	Pd(2)−S(4)−Pd(4)	106.4(3)	N(2)−Pt(2)−C(21)	81.5(2)	Pt(2)−S(4)−Pt(4)	111.90(6)
S(2)−Pd(3)−S(3)	100.5(2)	Pd(2)−S(4)−C(4)	104.2(8)	S(2)−Pt(3)−S(3)	98.71(5)	Pt(2)−S(4)−C(4)	105.29(19)
S(2)−Pd(3)−C(31)	95.8(7)	Pd(4)−S(4)−C(4)	94.5(8)	S(2)−Pt(3)−C(31)	96.06(17)	Pt(4)−S(4)−C(4)	93.7(2)
S(3)−Pd(3)−N(3)	82.7(6)	Pd(1)−N(1)−N(11)	127.0(14)	S(3)−Pt(3)−N(3)	83.56(14)	Pt(1)−N(1)−N(11)	122.8(4)
N(3)−Pd(3)−C(31)	80.9(9)	Pd(1)−N(1)−C(10)	118(2)	N(3)−Pt(3)−C(31)	81.7(2)	Pt(1)−N(1)−C(10)	116.8(4)
S(1)−Pd(4)−S(4)	99.4(2)	Pd(2)−N(2)−N(21)	125.6(13)	S(1)−Pt(4)−S(4)	98.80(5)	Pt(2)−N(2)−N(21)	123.6(4)
S(1)−Pd(4)−C(41)	96.1(6)	Pd(2)−N(2)−C(20)	116(2)	S(1)−Pt(4)−C(41)	96.73(17)	Pt(2)−N(2)−C(20)	117.0(4)
S(4)−Pd(4)−N(4)	82.8(6)	Pd(3)−N(3)−N(31)	123.9(14)	S(4)−Pt(4)−N(4)	83.10(14)	Pt(3)−N(3)−N(31)	123.9(4)
N(4)−Pd(4)−C(41)	81.6(8)	Pd(3)−N(3)−C(30)	117(2)	N(4)−Pt(4)−C(41)	81.2(2)	Pt(3)−N(3)−C(30)	117.3(4)
Pd(1)−S(1)−Pd(4)	109.9(2)	Pd(4)−N(4)−N(41)	123.3(14)	Pt(1)−S(1)−Pt(4)	112.13(6)	Pt(4)−N(4)−N(41)	124.2(4)
Pd(1)−S(1)−C(1)	93.5(8)	Pd(4)−N(4)−C(40)	116(2)	Pt(1)−S(1)−C(1)	93.80(18)	Pt(4)−N(4)−C(40)	116.7(4)

ligand, and the presence of a new band at 692 cm^{-1} in **2**, at 697 cm^{-1} in **3**, and at 700 cm^{-1} in **4** assignable to ν(C−S) indicate coordination via the sulfur atom in the thiol form.[12] The IR spectrum of compound **1** shows three absorptions for the stretching ν(NH) mode while complexes **2**, **3**, and **4** show only two bands (see the Experimental Section). These facts suggest that the ligand has been deprotonated and coordinated in the thiol form in both complexes.[12]

The low solubility of **2** in $CDCl_3$ made it necessary to record the ^1H and ^{13}C NMR spectra in DMSO-d_6. All of the NMR measurements were recorded immediately in order to avoid the interconversion reaction between **2** and **3** (see below). The ^1H NMR parameters for compound **1** and the complexes **2**, **3**, and **4** are depicted in Table 3.

The orthometalation of the *p*-isopropylphenyl ring is evident from the absence of the AA′BB′ system and the presence only of three aromatic protons. Usually, ortho and para protons, with respect to the palladium atom, should be more affected by the metalation.[10] In complex **2**, we observed the deshielding of the ortho proton, H4′ (7.37 ppm), and the carbon atoms, C4′ and C6 (at 130.65 and 147.41 ppm, respectively), which should be related with the electrophilicity of the metal.[13] The upfield shift observed for H4 proton and its corresponding carbon atom, C4, para to the palladium atom and unaffected by steric interactions, could be due primarily to the flow of charge from the electron-rich (d^8) metal atom into the aromatic ring (π-back-bonding).[14] The strong shielding effect at H5, meta to the Pd−C bond, which should be less affected by the cyclometalation, is probably due to interactions through the space of overlying aromatic rings.[14] This must be a consequence of the structure of these complexes, confirmed by X-ray diffraction. We also observed the disappearance of the signal at 11.39 ppm, corresponding to the NH group. This fact and the shielding effect produced in C8 carbon (177.95 ppm in **1** and 167.75 ppm in **2**) confirm the coordination through the sulfur atom in the thiol form of this complex. The signal corresponding to H7 bonded to the carbon of the azometinic group appears upfield shifted respect to the

Table 3. ^{1}H NMR Parameters δ (ppm) of the p-is. TSCN, **1**, and the Complexes **2**, **3**, and **4**[a]

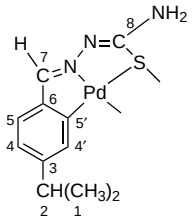

	1	2	4	4′	5	5′	7	NH	NH_2
1	1.19 d (6H) *J* (6.8)	2.89 sp (1H) *J* (6.8)	7.26[b] (2H)	eq H_4	7.69[b] (2H)	eq H_5	8.01 s (1H)	11.39 s (1H)	7.94 s (1H) 8.18 s (1H)
2	1.13 d (6H) *J* (6.9)	2.70 sp (1H) *J* (6.9)	6.84 dd (1H) *J* (1.4, 7.6)	7.37 d (1H) *J* (1.4)	7.08 d (1H) *J* (7.6)		7.57 s (1H)		6.88 s.br (2H)
3	1.22 d (3H) *J* (6.9)	2.72 sp (1H) *J* (6.9)	6.67 dd (1H) *J* (1.5, 7.7)	7.17 d (1H) *J* (1.5)	6.51 d (1H) *J* (7.7)		6.60 s (1H)		6.62 s.br (2H)
4	1.26 d (3H) *J* (7.1) 1.23 d (3H) *J* (7.1)	2.80 sp (1H) *J* (7.1)	6.67 d (1H) *J* (7.5)	7.27 s (1H)	6.55 d (1H) *J* (7.5)		6.63 s (1H)		6.73 s.br (2H)

[a] The numbers in parentheses correspond to J (^{1}H−^{1}H) in Hz. [b] AA′BB′ system. s = singlet, s.br = singlet broadened, d = doublet, sp = septet, dd = double doublet.

ligand ($\Delta\delta = -0.44$ ppm) which should be related with metal-to-ligand back-bonding, in agreement with the chemical shift found in other endo complexes (i.e. C=N group is part of the chelate ring).[10,15] The protons of the NH_2 group have also changed in the complex with respect to those of the ligand. This group in the ligand appears as two singlets at 7.94 and 8.18 ppm, whereas the complex **2** spectrum shows only a singlet at 6.88 ppm. When the ^{1}H NMR spectrum of the ligand is recorded in $CDCl_3$, only one signal can be observed for these protons, which indicates these protons are chemically equivalent. In the ^{13}C NMR spectrum, C5′, which is directly joined to the palladium atom, is strongly deshielded compared with the normal range for the aromatic carbons (127.46 ppm in **1** and 165.67 ppm in **2**), indicating that the cyclometalation has taken place on this carbon.[5]

Similar to that found in the ^{1}H NMR spectra of complex **2**, the aromatic region of the ^{1}H NMR spectrum of complex **3** shows the absence of the AA′BB′ system and the presence of three aromatic protons, which indicates that the cyclometalation has been produced in this complex. However all protons appear more upfield shifted than in complex **2**. This effect is higher for H5 ($\Delta\delta = -0.61$ and -1.18 ppm for **2** and **3**, respectively) and H7 ($\Delta\delta = -0.44$ and -1.41 ppm for **2** and **3**, respectively). The disappearance of the NH signal and the upfield shift produced in the C8 carbon (177.95 ppm in **1** and at 167.37 ppm in **3**) again confirm that the coordination through the sulfur atom in the thiol form has been produced. The strong deshielding found in C5′ (127.46 ppm in **1** and 164.87 ppm in **3**) confirms that the cyclometalation has been produced on this carbon.[5]

The ^{1}H NMR spectra of complex **2** in DMSO shows after 24 h that, besides the peaks corresponding to this complex, a set of peaks appears which are assigned to complex **3**. The ratio of this species is 1:1 (see Figure 3). When compound **3** is dissolved in $CDCl_3$, a yellow precipitate is formed after 24 h. This solid precipitate can be separated by filtration and corresponds to compound **2** as can be deduced from the ^{1}H NMR spectra in DMSO. This proves the interconversion of both isomers in solution.

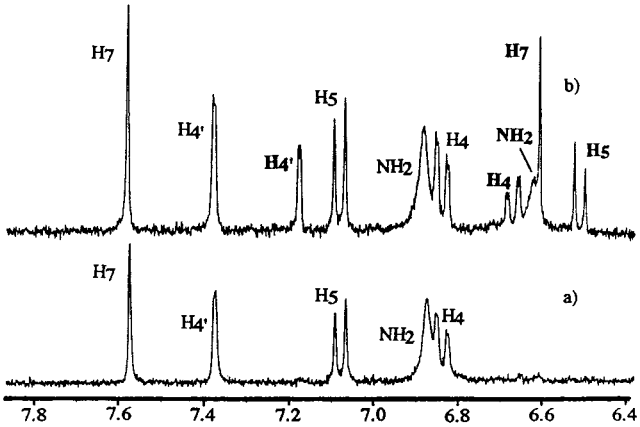

Figure 3. Aromatic region of the ^{1}H NMR spectrum of complex **2** along time: (a) $t = 0$, (b) $t = 24$ h.

The ^{1}H NMR spectra of platinum complex **4** are very similar to those of the palladium isomer **3**. Moreover, complex **4** shows the typical ^{13}C NMR spectra of a cyclometalated complex (see the Experimental Section).

Cytotoxic Activity. Due to the fact that thiosemicarbazones exhibit biological activity against viruses, fungi, pathogens, and several type of tumors[16] and in view that some cyclometalated complexes could be regarded as potential antitumor drugs,[6] we have tested the cytotoxic activity of compounds **2**, **3**, and **4**.

Table 4 shows the IC_{50} values of compounds **2**, **3**, **4**, *cis*-DDP, and the p-is.TSCN ligand against several tumor lines sensitive to *cis*-DDP (Jurkat, Hela, 3T3), resistant to *cis*-DDP (Pam-Ras and Glioma prymary cultures derived from two cancer patients) and normal cells (Pam). It may be seen that complex **2** has IC_{50} values between 3 and 62 μM, depending on the tumor cell line, being in general more active than complex **3** that exhibits IC_{50} values between 6 and 50 μM. Moreover, the platinum analogue **4** shows an intermediate cytotoxicity relative to that of isomers **2** and **3** displaying IC_{50} values ranging from 9 to 54 μM.

Table 4. IC_{50} Values Obtained for Compounds **1**, **2**, **3**, **4**, *cis*-DDP, Etoposide, and Adriamycin against Several Tumor and Normal Cell Lines

	IC_{50} (μM) ± SD						
compd	PAM-RAS	GLIOMA # 108	GLIOMA # 112	JURKAT	HeLa	3T3	PAM
1	65 ± 2	98 ± 5	75 ± 3	9 ± 0.4	78 ± 3	97 ± 5	88 ± 6
2	5 ± 0.4	62 ± 3	35 ± 1	7 ± 0.3	4 ± 0.1	3 ± 0.2	8 ± 0.3
3	37 ± 3	40 ± 3	50 ± 2	6 ± 0.3	45 ± 3	32 ± 0.6	150 ± 9
4	9 ± 0.6	54 ± 2	27 ± 2	7 ± 0.5	20 ± 3	21 ± 3	30 ± 3
cis-DDP	165 ± 5	86 ± 3	120 ± 6	22 ± 3	7 ± 0.5	35 ± 2	164 ± 8
etoposide	136 ± 10	76 ± 2	62 ± 4				180 ± 12
adriamycin	156 ± 11						150 ± 5

Table 4 also shows that compounds **2**, **3**, and **4** are approximately 33 times, 4 times, and 18 times, respectively, more active than *cis*-DDP in the *cis*-DDP resistant cell line Pam-Ras. Compound **3** is the one that has the best therapeutic index when comparing the cytotoxicity of the compounds in normal Pam cells (IC_{50} values of 8, 150, and 30 μM, respectively) versus transformed Pam-Ras cells (IC_{50} values of 5, 37, and 9 μM, respectively). Moreover, complexes **2**, **3**, and **4** exhibit higher cytotoxic activity than the clinically used drugs etoposide and adriamycin in this *cis*-DDP resistant cell line. On the other hand, compounds **2**, **3**, and **4** display notorious cytotoxic activity against two primary culture of glioma cells (IC_{50}values of 62 and 35 μM for compound **2**, 40 and 50 μM for compound **3**, and 54 and 27 μM for compound **4**) in which *cis*-DDP has poor cytotoxicity (IC_{50} = 86 and 120 μM, respectively) and etoposide has mild cytotoxicity (IC_{50} = 76 and 62 μM, respectively). It should be pointed out that etoposide is one of the drugs currently used for the treatment of brain tumors.[17] The data of Table 4 also indicates that the p-is.TSCN ligand has in general poor cytotoxic activity except in Jurkat cells in which it exhibits and IC_{50} = 9 μM.

Altogether, the above suggest that the covalent binding of *cis*-Pd(II) and *cis*-Pt(II) centers to the p-is.TSCN results in tetrameric cyclometalated compounds with new spectra of cytotoxic activity. Thus, from the anticancer screening data presented in Table 4 it may be concluded that complexes **2**, **3**, and **4** may be considered as potential antitumor agents particularly in view of the fact that they are active in tumor cells in which *cis*-DDP and etoposide have poor or moderate cytotoxic activity. The fact that complexes **2**, **3**, and **4** display significant cytotoxic activity against tumor cell lines resistant to *cis*-DDP indicates that these compounds should have a biochemical mechanism of action different from that of *cis*-DDP.

Analysis of the Interaction of Compounds 2, 3, and 4 with DNA. Since the cytotoxicity assays indicate that compounds **2**, **3** and **4** should have a biochemical mechanism of action different from that of *cis*-DDP and, on the other hand, it is well-known that the pharmacological target of *cis*-DDP is DNA,[18] we have analyzed the interaction of these compounds with DNA.

Circular Dichroism Spectra of Compound:DNA Complexes. The effect of binding of compounds **2**, **3** and **4** on DNA secondary structure was determined by CD spectroscopy of compound:DNA complexes. The CD spectra and the wavelength at which the maximum and minimum values of elipticity [θ] occur in control DNA and in DNA incubated with compounds **2**, **3, 4**, and *cis*-DDP at r_i = 0.01 for 24 h are shown in Figure 4. It can be observed that the CD spectra of compound **2**:DNA and compound **3**:DNA are superimposed. The maximum value of elipticity of the positive band at 283 nm in native DNA decreases from 1000 θ units to 935 θ units in both compound **2**:DNA and compound **3**:DNA complexes. These changes in elipticity values are accompanied by a bathochromic effect in the maximum of the positive band which is located at 281 nm. In compound **4**:DNA complexes the maximum value of ellipticity also decreases relative to native DNA and is located at 283 nm having a θ value of 839 units. In *cis*-DDP:DNA complexes the maximum value of elipticity of the positive band is located at 281 nm having a θ value of 948 units. The minimum value of elipticity of the negative band present in native DNA at 240 nm increases from −600 θ units to −1000 θ units in compound **2**:DNA and compound **3**:DNA complexes. Moreover, a small bathochromic effect is induced in the minimum value of elipticity of the negative band which is located at 241 nm. In contrast, compound **4** induces a decrease in the minimum of elipticity of the negative band having a value of −293 θ units at 240 nm. In *cis*-DDP:DNAcomplexes the elipticity of the negative band also decreases, having a θ value of −500 units at 241 nm. The differences observed in the negative band of the CD spectrum of compound **2**:DNA and compound **3**:DNA complexes relative to compound **4**:DNA complexes indicate that in the cyclopalladated compounds **2** and **3** the palladium atom produces on DNA secondary structure conformational changes which are different

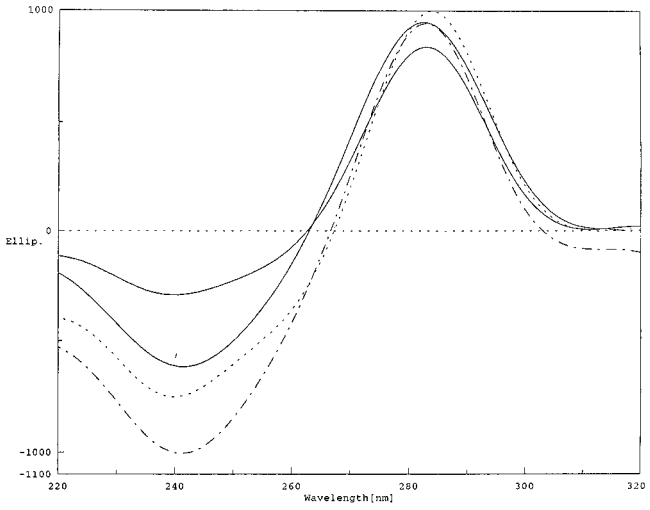

Figure 4. CD spectra of control CTDNA (—) and of CT DNA incubated with compounds **2** and **3** (—•—), compound **4** (—) and *cis*-DDP (- - -) at r_i = 0.01 for 24 h.

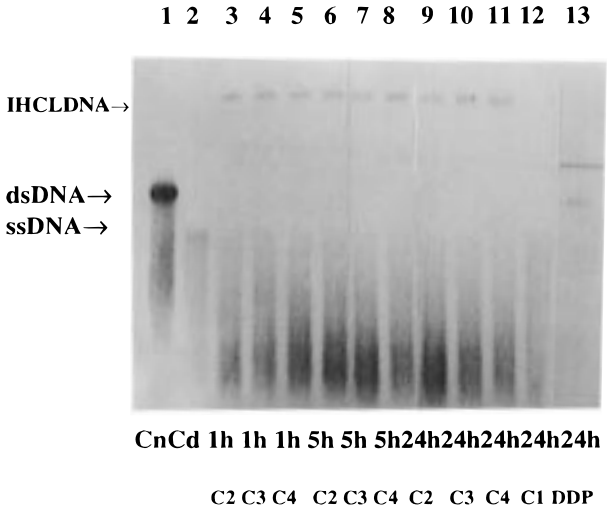

Figure 5. Pattern of single- and double-stranded DNA after melting of compound **2:**pBR322 DNA, compound **3**:pBR322 DNA, and compound **4**:pBR322 complexes, formed after incubation of linear pBR322 plasmid DNA with compounds **2**, **3**, and **4** at $r_i = 0.01$ (Cn, native DNA; Cd, denaturated DNA; IHCLDNA, interhelical cross-linked DNA; dsDNA, double-stranded DNA; ssDNA, single-stranded DNA; **C1**, (p-is.TSCN), *p*-isopropylthiosemicarbazone ligand; DDP, cisplatin.

from those induced by the platinum atom in the cycloplatinated analogue **4**. On the other hand, it is interesting to point out that a "tailing effect" appears at 315 nm in the CD spectrum of compound **2**:DNA and compound **3**:DNA complexes having a θ value of -109 units. In the CD spectrum of compound **4**:DNA is also observed a "tailing effect" at 315 nm but with a θ value of $+37$ units. This "tailing effect" is absent in *cis*-DDP:DNAcomplexes and may be attributed to the formation of DNA aggregates due to DNA interhelical cross-links formed by the metal.[19]

Interhelical Cross-Link Formation. To find out whether the "tailing effect" observed in the CD spectrum of compound **2:**DNA, compound **3**:DNA and compound **4**:DNA complexes may be due to interhelical cross-link formation, we have carried out experiments to detect the presence of DNA aggregates after DNA melting. Figure 5 shows the pattern of stranded DNA bands after melting of compound **2:**DNA, compound **3**:DNA, and compound **4**:DNA complexes formed at a $r_i = 0.01$ for 1, 5, and 24 h of incubation. As expected, native pBR322 melted DNA migrates as a smear which corresponds to single stranded DNA form (lane 2). Also, melted compound **2**:pBR322 DNA, melted compound **3**:pBR322 DNA, melted compound **4**:pBR322 DNA, and melted p-is.TSCN:pBR322 DNA migrates as a smear of single DNA strand (middle of Figure 5; lanes 3 to 11 and lane 12, respectively). Surprisingly, however, a fraction of high molecular weight DNA bands retained in the agarose wells were observed at all the periods of incubation of pBR322 DNA with compounds **2**, **3** and **4** (top of Figure 5, lanes 3−11) as an indication that bands of unmelted DNA were forming aggregates due to interhelical cross-link formation of the compounds with several double-stranded DNA molecules.[20] Thus, it seems that, in compound **2**:DNA, compound **3**:DNA, and compound **4**:DNA complexes, extensive interhelical cross-linking of DNA fragments results in a DNA mixture of high molecular weight unable to penetrate through the agarose gel matrix. The detection of DNA interhelical cross-links using DNA denaturing techniques followed by agarose gel electrophoresis has been previously reported in *cis*-Pt dimers.[20] The densitometric analysis of the fractions of DNA bands retained in the agarose wells indicated that the amount of interhelical cross-linked DNA produced by compounds **2**, **3**, and **4** after 1, 5, and 24 h of incubation is almost the same being approximately 25% of total DNA. Moreover, it is interesting to note that both cisplatin and the p-is.TSCN ligand did not produce DNA bands at the top of the gel as an indication that they are unable to form DNA interhelical cross-links. On the other hand, compounds **2**, **3**, and **4** did not seem to induce DNA interstrand cross-links because the double-stranded pBR322 DNA band which appears in control unmelted DNA (lane 1) is not observed in compound **2**:DNA, compound **3**:DNA, and compound **4**:DNA complexes (lanes 3−11). On the contrary, *cis*-DDP induces the formation of some interstrand cross-links in pBR322 DNA because a DNA band corresponding to double stranded unmelted pBR322 DNA is observed in *cis*-DDP:DNA complexes (lane 13). Thus, the above results support the findings previously observed by CD spectroscopy and indicates that, in contrast with *cis*-DDP, compounds **2**, **3**, and **4** form DNA interhelical cross-links.

Altogether, the data obtained from the analysis of the interaction of compounds **2**, **3** and **4** with DNA indicate that these tetrameric complexes share a unique feature, namely, the formation of DNA interhelical cross-links. Due to the fact that these compounds are active in *cis*-DDP resistant cell lines and that, on the other hand, *cis*-DDP is unable to form DNA interhelical cross-links, it is tentative to speculate about the possibility that part of the biochemical mechanism of action of these novel tetranuclear cyclometalated compounds may be due to DNA interhelical cross-links formation. In fact, it has been previously reported that bis-Pt complexes, which also form DNA interhelical cross-links, are active in tumor cells resistant to *cis*-DDP.[20]

Since the cytotoxic activity of compound **4** is intermediate between that of compounds **2** and **3** and, moreover, *cis*-DDP does not form interhelical cross-links, we think that in compounds **2**, **3**, and **4** the maintenance of the oligomeric structure is essential to produce this type of DNA adducts. Taking into account that in compounds **2**, **3**, and **4** the Pd or Pt atoms adopt a square-planar structure, we postulate that a nucleophilic attack could be directed from some nitrogens of the bases (i.e., N7/N3 of guanine residues) of different DNA molecules toward two or more metallic centers within the cyclometalated tetramer without breaking up the cluster. Thus, the preservation of the clustered structure would be in agreement with the results obtained in the present paper indicating that compounds **2**, **3**, and **4** form DNA aggregates by means of DNA interhelical cross-links.

Experimental Section

Infrared spectra were recorded in Nujol mulls on CsI windows and KBr pellets in the 4000−200 cm^{-1} range with a Perkin-Elmer model 283 spectrophotometer. NMR spectra were recorded on a Brucker AMX-300 (300 MHz) spectrometer in DMSO-d_6 solution. Elemental analyses were performed on

Table 5. Crystal Data and Structure Refinement for Complex **2** and Complex **4**

	complex **2**	complex **4**
empirical formula	$C_{46}H_{56}N_{12}O_2Pd_4S_4$	$C_{47.25}H_{60.50}Cl_{4.50}N_{12}OPt_4S_4$
formula weight	1362.97	1880.69
temperature, K	293(2)	160(2)
wavelength, Å	0.71069	0.71073
crystal system	monoclinic	monoclinic
space group	*C*2/*c*	*C*2/*c*
unit cell dimensions	$a = 25.485(2)$ Å	$a = 25.873(2)$ Å
	$b = 19.524(3)$ Å	$b = 19.5053(14)$ Å
	$c = 24.298(5)$ Å	$c = 24.090(2)$ Å
	$\alpha = 90°$	$\alpha = 90°$
	$\beta = 101.62(1)°$	$\beta = 101.305(2)°$
	$\gamma = 90°$	$\gamma = 90°$
volume, Å^3	11842(3)	11921(2)
Z	8	8
density (calcd), mg/m^3	1.529	2.095
absorption coeff, mm^{-1}	1.38	9.746
F(000)	5440	7100
crystal size	0.42 × 0.15 × 0.10 mm	0.36 × 0.12 × 0.10 mm
θ (deg) range for data collection	1.32−25.00	1.61−28.40
index ranges	$0 \le h \le 30$, $0 \le k \le 23$, $-28 \le l \le 28$	$-14 \le h \le 34$, $-26 \le k \le 24$, $-31 \le l \le 29$
reflections collected	10408	36395
independent reflections	10408	13646 [$R_{int} = 0.0340$]
reflexion with $I > 2\sigma(I)$	4115	10478
absorption correction	empirical	semiempirical
max. and min. transmission	1.102 and 0.987	0.460 and 0.287
structure solution	direct methods	direct methods
refinement method	full-matrix least-squares on F^2	full-matrix least-squares on F^2
data/parameters	4115/594	13646/0/682
goodness-of-fit on *F*	1.09	1.052
final *R* indices [$I > 2\sigma(I)$]	R1 = 0.055, wR2 = 0.077	R1 = 0.0319, wR2 = 0.0697
R′ indices (all data)	R1 = 0.105, wR2 = 0.125	R1 = 0.0529, wR2 = 0.0769
largest diff peak and hole, e Å^{-3}	1.442 and −1.118	1.569 and −1.302

a Perkin-Elmer 2400 series II microanalyzer. FAB mass spectra (*m*/*z*) were obtained with V.G. AUTOSPECT high-resolution spectrometer. This experimental part was achieved by L-SIMS techniques using m-NBA. Spectra were assigned on the basis of chemical shift and spin−spin coupling information and by heteronuclear correlation two-dimensional NMR spectroscopy.[21]

All solvents were purified, prior to use, by standard methods. Palladium(II) acetate was purchased from Aldrich.

Synthesis of *p*-Isopropylbenzaldehyde Thiosemicarbazone, 1. The ligand p-is.TSCN, **1**, was synthesized as previously reported.[22] Anal. ($C_{11}H_{15}N_3S$). IR: ν_{max} 3415, 3274, 3160, 1594, 829, 820 cm^{-1}. ^{13}C NMR: 23.69 (C1), 33.49 (C2), 142.84 (C3), 126.71 (C4), 127.46 (C5), 131.78 (C6), 150.64 (C7), 177.95 (C8) ppm.

Synthesis of Complexes 2 and 3. To *p*-isopropylbenzaldehyde thiosemicarbazone (221 mg, 1 mmol) in glacial AcOH (15 mL) under argon was added palladium(II) acetate (225 mg, 1 mmol) with stirring; the mixture was then heated (ca. 40 °C) for 24 h. The solvent was removed in vacuo, and the residue was purified by chromatography (SiO_2) with CH_2Cl_2 as eluent to remove any unchanged starting material. The elution with CH_2Cl_2/EtOH (100:1) yielded the yellow complex **2** (72%), and the orange complex **3** (15%) was obtained when the eluent was CH_2Cl_2/EtOH (100:5).

Yellow Complex 2, [Pd(p-is.TSCN)]$_4$. Anal. ($C_{46}H_{56}N_{12}O_2S_4Pd_4$). IR: ν_{max} 3474, 3279, 1625, 1579, 692 cm^{-1}. FAB-MS: 1303.1 (M^{3+}). ^{13}C NMR: 23.88 (C1), 34.05 (C2), 148.80 (C3), 122.90 (C4), 130.65 (C4′), 126.28 (C5), 165.67 (C5′), 147.41 (C6), 158.67 (C7), 167.75 (C8) ppm.

Dark Orange Complex 3, [Pd(p-is.TSCN)]$_4$. Anal. ($C_{44}H_{52}N_{12}S_4Pd_4$). IR: ν_{max} 3427, 3277, 1623, 1580, 697 cm^{-1}. FAB-MS: 1304.1 (M^{4+}). ^{13}C NMR: 24.19 (C1), 34.74 (C2), 149.41 (C3), 121.82 (C4), 131.49 (C4′), 127.50 (C5), 164.87 (C5′), 145.92 (C6), 161.01 (C7), 167.37 (C8) ppm.

Synthesis of Complex 4. To a solution of *p*-isopropylbenzaldehyde thiosemicarbazone (0.09 g, 0.40 mmol) in 4 mL of MeOH was added K_2PtCl_4 (0.17 g, 0.40 mmol), and the mixture was stirred at 23 °C for 15 days. The solvent was removed via rotatory evaporation. The residue was dispersed in Celite and purified by chromatography on a silica gel column with CH_2Cl_2 as eluent to remove any unchanged starting material. Upon further elution with CH_2Cl_2/EtOH (100:1), the tetranuclear complex $Pt_4C_{44}H_{52}N_{12}S_4$ (80%) was obtained. Crystallization was achieved by slow evaporation of a EtOH and CH_2Cl_2 solution.

Pale Orange Complex 4, ([Pt(p-is.TSCN)]$_4$·2.25·CH_2Cl_2·MeOH). Anal. ($C_{47.25}H_{60.50}Cl_{4.50}N_{12}OS_4Pt_4$): C, 30.18; H, 3.24; N, 8.94; S, 6.82. IR: ν_{max} 3433, 3373, 1611, 1583, 700 cm^{-1}. FAB-MS: 1657.7 (M^+). ^{13}C NMR: 23.67 (C1), 34.74 (C2), 150.94 (C3), 121.05 (C4), 129.43 (C4′), 128.29 (C5), 154.16 (C5′), 145.14 (C6), 162.10 (C7), 164.97 (C8) ppm.

Structural Determination and Refinement of Complex 2. A yellow single crystal obtained by slow evaporation from a $CHCl_3$ solution was mounted on an Enraf-Nonius CAD4 four-circle diffractometer and used for data collection. Information concerning crystal parameters and structure refinement is summarized in Table 5. Intensity data were corrected for Lorentz polarization and absorption[23] effects. Atomic scattering factors and anomalous dispersion terms were taken from ref 24. The structure was solved by direct methods[25] and refined (on F) by full-matrix least-squares using the X-RAY 76 program package.[26] Non-hydrogen atoms were refined anisotropically, except those belonging to the acetic acid solvate which were refined isotropically due to their considerable high thermal motion. The largest peak in the final Fourier-difference map of 1.44 e Å^{-3} high was located in the vicinity of the solvate molecule. A convenient weighting scheme[27] was used in final cycles of refinement to obtain flat dependence in $<\omega\Delta^2F>$ vs $<F_o>$ and $<\sin\theta/\lambda>$. The molecular plots were drawn with the PLATON program.[28]

Structural Determination and Refinement of Complex 4. An orange single crystal obtained by slow evaporation from a CH_3OH/CH_2Cl_2 solution was mounted on a Siemens SMART CCD diffractometer and used for data collection. Information concerning crystal parameters and structure refinement is summarized in Table 5. Intensity data were corrected for Lorentz polarization and absorption effects. The structure was solved by direct methods using the SHELXS-86[29] program and refined by full-matrix least-squares method

on F^2 using the SHELXL-96[30] program package. All non-hydrogen atoms were refined anisotropically.

Reagents and Compounds. The 100-mm culture and microwell plates were obtained from NUNCLON (Roskilde, Denmark). MTT was purchased by Sigma Chemical Co.; FCS was supplied by GIBCO-BRL; *cis*-DDP (*cis*-diamminedichloroplatinum(II)) and etoposide [(9-[4,6-*O*-ethylidene-β-D-glucopyranosyl)oxy]-5,8,8a, 9-tetrahydro-5-(4-hydroxy-3,5-dimethoxyphenyl)furo[3′,4′:6,7]naphthol[2,3-*d*]-1,3-dioxol-6(5a*H*)-one; 4′-demethyl epipodophyllotoxin, 9-[4,6-*O*-ethylidene-β-D-glucopyranoside] were purchased from Sigma Chemical Co. Adriamycin (doxorubicin) [(8-*cis*)-10-[(3-amino-2,3,6-trideoxy-α-L-*lyxo*-hexopyranosyl)oxy]-7,8,9,10-tetrahydro-6,8,11-trihydroxy-8-(hydroxyacetyl)-1-methoxy-5,12-naphthacenedione] was purchased from Tedec-Meiji Farma, S.A as doxorubicin chlorhydrate. *cis*-DDP and Adriamycin were dissolved in PBS, and etoposide was dissolved in ethanol. Compounds **1**, **3**, and **4** were dissolved in ethanol, and compound **2** was dissolved in DMSO. Stock solutions of the compounds at a concentration of 1 mg/mL were freshly prepared before use.

Cell Lines and Culture Conditions. Jurkat (acute T-cell leukemia line) cells were cultured in RPMI 1640 medium supplemented with 10% FCS (foetal calf serum), 2 mM glutamine, 100 units/mL penicillin, and 100 mg/mL streptomycin at 37 °C in an atmosphere of 95% of air and 5% of CO_2. Hela (cervix epithelial carcinoma line) and NIH 3T3 (transformed murine fibroblasts) cells were cultured in DMEM medium supplemented with 10% FCS and 10% of new born calf serum, respectively, together with 2 mM glutamine, 100 units/mL penicillin, and 100 mg/mL streptomycin at 37 °C in an atmosphere of 95% of air and 5% of CO_2. Pam (murine keratinocytes) and Pam-Ras (murine keratinocites transformed with the H-ras oncogene and resistant to *cis*-DDP) were cultured in DMEM medium supplemented with 10% FCS and 2 mM glutamine, 100 units/mL penicillin, and 100 mg/mL streptomycin at 37 °C in an atmosphere of 95% of air and 5% of CO_2. Primary cultures of glioma cells (obtained from biopsies of two different cancer patients of Hospital "La Paz" of Madrid, glioma 108 and glioma 112) were cultured in MEM medium supplemented with 10% FCS, 2 mM glutamine, 100 units/ml penicillin, and 100 mg/mL streptomycin in the abovementioned conditions. The cultures of tumor cells (Jurkat, Hela, 3T3, Pam-Ras and Glioma) were passaged three-times per week showing a doubling time between 16 and 24 h depending on the cell line. Normal murine keratinocytes were passaged twice weekly showing a doubling time of about 48 h.

Drugs Cytotoxicity. Cell proliferation in compound-treated cultures was evaluated by using a system based on the tetrazolium compound MTT (3-[4,5-dimethylthiazol-2-yl]-2,5-diphenyltetrazolium bromide) which is reduced by living cells to yield a soluble formazan product that can be assayed colorimetrically. Cells were platted in 96-well sterile plates, at a density of 10^4 cells/well in 100 μL of medium, and were incubated for 3−4 h. Compounds were added to final concentrations from 0 to 100 μM, in a volume of 100 μL/well. Twenty-four hours later, 50 μL of a freshly diluted MTT solution (1/5 in culture medium) was added to a concentration of 1 mg/mL into each well, and the plates were incubated for 5 h at 37 °C in a humidified 5% CO_2 atmosphere. After that, cell survival was evaluated by measuring the absorbance at 520 nm, using a Whittaker Microplate Reader 2001. IC_{50} values were calculated from curves constructed by plotting cell survival (%) versus compound concentration (μM). All experiments were made in quadruplicate. In control experiments it was observed that solutions containing 10% of DMSO or 10% of ethanol in culture medium did not have any effect on cell survival. These were the highest concentrations of DMSO or ethanol present in the 96-microwell culture plates after adding the compounds.

Formation of Compound:DNA Complexes. The formation of the compound:DNA complexes was done by addition to CT DNA (Calf Thymus DNA, Sigma Co., and pBR322 plasmid DNA, Sigma Co.) of aliquots of each of the complexes at different concentrations in TE buffer (10 mM Tris·HCl, 0.1 mM EDTA, pH 7.4). The amount of compound added to the DNA solution was expressed as r_i (the input molar ratio of Pd, Pt or p-is.TSCN to nucleotides). The mixture was incubated at 37 °C for various periods of time as indicated below. The fraction of unreacted compounds was separated from the mixture by precipitation of the DNA with 2.5 volumes of ethanol and 0.3 M sodium acetate, pH 4.8.

Interstrand and Interhelical Cross-Link Assays. To linearize pBR322 plasmid, DNA was digested in 150 mM NaCl with 10 units/μg DNA of Bam HI at 37 °C for 4 h. pBR322 DNA was 3′-end labeled by incubation with 2.5 μCi/μg DNA of [α-^{32}P]dCTP and 1.25 units/μg DNA of Klenow fragment of *E. coli* DNA polymerase I for 30 min at room temperature. The reaction was stopped by heating at 70 °C for 5 min. Unincorporated radioactivity was removed by passing the labeling reaction through a Sephadex G-50 column. Sonicated CT DNA was added to the eluted solution of labeled pBR322 DNA to a final DNA concentration of 180 μg/mL. DNA at a concentration of 90 ng/mL was incubated with the compounds in Bam HI buffer (150 mM NaCl) for 1, 5, and 24 h at r_i = 0.01. Aliquots of 10 μL were removed after the different incubation times, and the reaction was ended by addition of an equal volume of loading dye (90% formamide, 10 mM EDTA, 0.1% xylene cyanol, and 0.1% bromophenol blue). The DNA was melted for 10 min at 90 °C, and the samples were chilled on ice prior to loading onto an 1.5% agarose gel. Agarose gel electrophoresis was carried out in TAE buffer (Tris-acetate 40 mM, EDTA 2 mM, pH 8.0) at 20 V for 16 h. Gels were dried and autoradiographed. Band quantitation was made using a Molecular Dynamics 300A densitometer.

Circular Dichroism Spectroscopy. The CD spectra were performed in a 1-cm rectangular quartz cell in a JASCO J-600 spectropolarimeter attached to a temperature programmer using a computer for spectral subtraction and noise reduction. The CD analysis was done at 37 °C. Each sample was scanned twice in a range of wavelengths between 220 and 320 nm. The generated CD spectra represent the mean of three independent scans. The data are expressed as mean residue molecular elipticity [θ] in deg × cm^{-1} × $dmol^{-1}$.

Acknowledgment. This work was supported by the CICYT grant (SAF96-0041). An Institutional grant from Fundación Ramón Areces is also acknowledged. We also thank Dr. Ramón y Cajal from Clinica "Puerta de Hierro" of Madrid and Dr. Marta Izquierdo from Centro de Biología Molecular "Severo Ochoa" of Madrid for their kind gifts of Pam, Pam-Ras and Glioma cells, respectively. We also thank Eva Irene Montero Véliz for her collaboration in the cytotoxicity assays.

Supporting Information Available: Atomic coordinates and equivalent isotropic displacement parameters, anisotropic displacement parameters and hydrogen coordinates and isotropic displacement parameters for complex **2** and complex **4** (17 pages). Ordering information is given on any current masthead page.

References

(1) (a) Dobek, A. S.; Klayman, D. L.; Dickson, E. T.; Scovill, J. P.; Oster, C. N. Thiosemicarbazones of 2-Acetylpyridine, 2-Acetylquinoline, 1- and 3-Acetylisoquinoline and Related Compounds as Inhibitors of Clinically Significant Bacteria *In Vitro*. *Arzneim. Forsch.* **1983**, *33*, 1583. (b) Scovill, J. P.; Klayman, D. L.; Franchino, C. F. 2-Acetylpyridine Thiosemicarbazones Complexes With Transition Metals as Antimalarial and Antileukemic Agents. *J. Med. Chem.* **1982**, *25*, 1261. (c) Klayman, D. L.; Scovill, J. P.; Mason, C. J.; Bartosevich, J. F.; Bruce, J.; Lin, A. 2-Acetylpyridine Thiosemicarbazones. 6. 2-Acetylpyridine and 2-Butyrylpyridine Thiosemicarbazones as Anti-leukemic Agents. *Arzneim. Forsch.* **1983**, *33*, 909. (d) Shipman, C., Jr.; Smith, S. H.; Drach, J. C.; Klayman, D. L. Thiosemicarbazones of 2-Acetylpyridine, 2-Acetylquinoline, 1-Acetylisoquinoline, and Related-Compounds as Inhibitors of Herpes-simplex Virus *In Vitro* and In a Cutaneous Herpes Guinea-pig Model. *Antiviral*

Res. **1986**, *6*, 197. (e) Pandeya, S. N.; Dimmock, J. R. Recent Evaluations of Thiosemicarbazones and Semicarbazones and Related Compounds for Antineoplastic and Anticonvulsant Activities. *Pharmazie* **1993**, *48*, 659.

(2) (a) Aravindakshan, K. K.; Nair, C. G. R. Preparation and Characterization of Solid Complexes of 2-Furaldehyde Thiosemicarbazone with Some Transition Metal Ions. *Indian J. Chem., Sect. A* **1981**, *20*, 684. (b) Crim, J. A.; Petering, H. G. Antitumor Activity of Cu(II)KTS, the Cu(II) Chelate of 3-Ethoxy-2-oxobutyraldehyde Bis(thiosemicarbazone). *Cancer Res.* **1967**, *27*, 1278. (c) Petering, D. H.; Antholine, W. E.; Saryan, L. A. Metal Complexes as Antitumor Agents, α-N-Heterocyclic carboxaldehyde Thiosemicarbazones. In *Anticancer and Interferon Agents. Syntheses and Properties*; Ottenbrite, R. H., Butler, G. B., Eds.; Marcel Dekker: New York, 1984; p 221. (d) Kovala-Demertzi, D.; Domopuolou, A.; Demertzi, M. Coordinating Properties of 2-Acetylpyridine Thiosemicarbazone. Palladium(II) Complexes with Neutral and Deprotonated Ligand. X-ray Structure of Bromo(2-Acetylpiridine Thiosemicarbazonato) Palladium(II). *Polyhedron* **1994**, *13*, 1917.

(3) (a) West, D. X.; Liberta, A. E.; Padhye, S. B.; Chikate, R. C.; Sonawane, P. B.; Kumbhar, A. S.; Yerande, R. G. Thiosemicarbazone Complexes of Copper(II): Structural and Biological Studies. *Coord. Chem. Rev.* **1993**, *123*, 49. (b) Campbell, M. J. M. Transitioin Metal Complexes of Thiosemicarbazide and Thiosemicarbazone. *Ibid.* **1975,** *15*, 279. (c) Wiles, D. M.; Gingras, B. A.; Suprunchuk, T. The C═S Stretching Vibration in the Infrared Spectra of Some Thiosemicarbazones. *Can. J. Chem.* **1967**, *45*, 469. (d) West, D. X.; Bain, G. A.; Butcher, J.; Jasinski, J. P.; Li, Y.; Pozdniakv, Y.; Valdés-Martínez, J.; Toscano, A. R.; Hernández-Ortega, S. Structural Studies of Three Isomeric Forms of Heterocyclic N4-Sustituted Thiosemicarbazones and Two Nickel(II) Complexes. *Polyhedron* **1996**, *15*, 665. (e) Bingham, A. G.; Bogge, H.; Muller, A.; Ainscoing, E. W.; Brodie, A. M. Synthetic, Spectroscopic, and X-ray Crystallographic Studies on Binuclear Copper(II) Complexes with a Tridentate NNS-bonding 2-Formylpyridine Thiosemicarbazone Ligand. The Characterization of Both Neutral and Deprotonated Co-ordinated Ligand Structures. *J. Chem. Soc., Dalton Trans.* **1987**, 493. (f) García-Tojal, J.; Urtiaga, M. K.; Cortés, R.; Lezama, L.; Arriortua, M. I.; Rojo, T. Synthesis, Structure, Spectroscopic and Magnetic Propierties of Two Copper(II) Dimers Containing Pyridin-2-carbaldehyde Thiosemicarbazonate (L), [{CuL(X)$_2$}] (X = Cl or Br). *Ibid.* **1994**, 2233.

(4) (a) Hingorani, S.; Agarwala, B. V. Structural Investigation of Pd(II) and Pt(II) Complexes with *o*-Vainillin Thiosemicarbazone and 4-Phenylthiosemicarbazone and Their Mixed Ligand Complexes. *Spectrosc. Lett.* **1990**, *23*, 1097. (b) Kovala-Demertzi, D.; Domopoulo, A.; Demertzis, M. A.; Valdés-Martínez, J.; Hernández-Hortega, S.; Espinosa-Pérez, G.; West, D. X.; Salberg, M. M.; Bain, G. A.; Bloom, P. D. Palladium(II) Complexes of 2-Acetylpyridine N4-Propyl, N4-Dipropyl- and 3-Hexamethyleneimyl Thiosemicarbazones with Potencially Interesting Biological Activity. Synthesis, Spectral Properties, Antifungal and In Vitro Antitumor Activity. *Polyhedron* **1996**, *15*, 2587.

(5) (a) García-Ruano, J. L.; López-Solera, I.; Masaguer, J. R.; Navarro-Ranninger, C.; Rodríguez, J. H.; Martínez-Carrera, S. Cyclometalation of N-(4-Methoxyphenyl)-α-benzoylidenamine with Palladium(II) Acetate. Evidence for a New Kind of Diastereoisomerism. *Organometallics* **1992**, *11*, 3013. (b) Navarro-Ranninger, C.; López-Solera, I.; Alvarez-Valdés, A.; Rodríguez-Ramos, J. H.; Masaguer, J. R.; García-Ruano, J. L.; Solans, X. Cyclometalated Complexes of Palladium(II) and Platinum(II) with N-Benzyl- and N−(Phenylethyl)-α-Benzoylidenamine. Delocalization in the Cyclometalated Ring as a Driving Force for the Orthometalation. *Ibid.* **1993**, *12*, 4104. (c) García-Ruano, J. L.; González, A. M.; López-Solera, I.; Masaguer, J. R.; Navarro-Ranninger, C.; Raithby, P. R.; Rodríguez, J. H. Enantiomerically Pure Palladacycles Derived from *β*-Ketosulfoxides. *Angew. Chem., Int. Ed. Engl.* **1995**, *34*, 1351.

(6) (a) Navarro-Ranninger, C.; López-Solera, I.; Pérez, J. M.; Masaguer, J. R.; Alonso, C. *In Vitro* Antitumor Activity of Two Isomeric Cyclopalladated Compounds Derived from Benzoylbenzylidenimines. *Appl. Organomet. Chem.* **1993**, *7*, 57. (b) Navarro-Ranninger, C.; López-Solera, I.; Pérez, J. M.; Rodríguez, J.; García-Ruano, J. L.; Raithby, P. R.; Masaguer, J. R.; Alonso, C. Analysis of Two Cycloplatinated Compounds Derived from N-(4-Methoxyphenyl)-α-benzoylbenzylidenamine. Comparison of the Activity of These Compounds with Other Isostructural Cyclopalladated Compounds. *J. Med. Chem.* **1993**, *36*, 3795. (c) Navarro-Ranninger, C.; López-Solera, I.; González, V. M.; Pérez, J. M.; Alvarez-Valdés, A.; Martín, A.; Raithby, P. R.; Masaguer, J. R.; Alonso, C. Cyclometalated Complexes of Platinum and Palladium with N-(4-Chlorophenyl)-α-benzoylbenzylidenamine. *In Vitro* Cytostatic activity, DNA Modification, and Interstrand Cross-Link Studies. *Inorg. Chem.* **1996**, *35*, 5181.

(7) (a) Teixidor, F.; Sánchez, G.; Lucena, N.; Escriche, L.; Kivekäs, R.; Casabó, J Palladium-promoted Benzothiophene Condensation in NS2 Ligands. *J. Chem. Soc., Chem. Commun.* **1992**, 163. (b) Braunstein, P.; Luke, M. A.; Tiripicchio, A.; Camellini, M. T. Reactions of [Pd$_2$(μ-dppm)$_2$Cl$_2$] with Electrophilic Complexes Complexes of Copper and Gold. Synthesis of the Pd$_4$ Cluster [Pd$_4$(μ-Cl)$_2$(μ-dppm)$_4$](PF$_6$)$_2$·2(CH$_3$)$_2$CO. *Angew. Chem., Int. Ed. Engl.* **1987**, *26*, 768. (c) Mimoun, H.; Charpentier, R.; Mitschler, A.; Fisher, J.; Weiss, R. Palladium(II) *tert*-Butyl Peroxide Carboxylates. New Reagents for the Selective Oxidation of Terminal Olefins to Methyl Ketones. On the Role of Peroxymetalation in Selective Oxidative Processes. *J. Am. Chem. Soc.* **1980**, *102*, 1047. (d) Yamaguchi, T.; Shibata, A.; Ito, T. A Chiral Tetranuclear Platinum(II) Cluster Complex, [Pt$_4$(O$_2$CMe)$_4$(pro)$_4$] (Hpro = L-proline) *J. Chem. Soc., Dalton Trans.* **1996**, 4031. (e) Gibson, D.; Lippard, S. J. Preparation and Structural Characterization of a Novel Hexanuclear Complex of Platinum(II) with 2-Aminoethanethiolate. *Inorg. Chem.* **1986**, *25*, 219.

(8) Espinet, P.; Alonso, M. I.; García-Herbosa, G.; Ramos, J. M.; Jeannin, Y.; Philoche-Levisalles, M. Double Oxidative Carbon−Carbon Coupling of a Dimeric Orthopalladated Amido Complex Leading to Redox-Active Tetrapalladia Units [Pd$_4$]$^{n+}$. *Inorg. Chem.* **1992**, *31*, 2501.

(9) (a) Kawamoto, T.; Kushi, Y. Crystal and Molecular Structure of Tetra-palladium Cluster with a C,N,S-Tridentate Ligand. *Chem. Lett.* **1992**, 1057. (b) Kawamoto, T.; Nagasawa, I.; Kuma, H.; Kushi, Y. Pd···H-C Interactions. Preparation and Structure of Orthometalated Tetranuclear Complexes of Palladium(II) and Platinum(II). *Inorg. Chem.* **1996**, *35*, 2427.

(10) (a) García-Ruano, J. L.; López-Solera, I.; Masaguer, J. R.; Monge, M. A.; Navarro-Ranninger, C.; Rodríguez, J. H. Reactivity of Acetate-bridged Cyclopalladated Complexes. ^{1}H and ^{13}C NMR studies of some monomeric derivatives of N-(4-Methoxyphenyl)-α-benzoylbenzilideneamine. *J. Organomet. Chem.* **1994**, *476*, 111. (b) Steel, P. J.; Caygill, G. B. Cyclometalated Compounds. II. Proton and Carbon-13 Nuclear Magnetic Resonance Spectral Assignments of Cyclopalladated Compounds. *J. Organomet. Chem.* **1987**, *327*, 101.

(11) (a) Adams, R. D.; Horvath, Y. T.; Segmuller, B. E.; Yang, L. W. Metal-induced Cleavage of Carbon−sulfur Bonds in Thiolato Ligands. Thermolysis of HOs3(CO)10(μ-SC6H5) under Carbon Monoxide Pressure. The Synthesis and Crystal and Molecular Structures of Os4(CO)13(μ3S) and Os5(CO)15(μ4S). *Organometallics* **1983**, *2*, 1301. (b) Ghilardi, C. A.; Midollini, S.; Sacconi, L. An Enneanuclear Nickel Sulfide with a Cofacial Bi-octahedral Geometry. X-ray Crystal Structure of [Ni9(μ4-S)3(μ3-S)6(PET3)6]-[BHP4]2 *J. Chem. Soc., Chem. Commun.* **1981**, 47. (c) Bodensieck, U.; Santiago, J.; Stoeckli-Evans, H.; Suss-Fink, G. Tetranuclear Ruthenium Clusters Containing a Pseudo-octahedral Ru4S2 Framework and Diaminocarbene Ligands. *J. Chem. Soc., Dalton Trans.* **1992**, 255.

(12) (a) Casas, J. S.; Sánchez, A.; Sordo, J.; Vázquez-López, A.; Castellano, E. E.; Zukermann-Schpector, J.; Rodríguez-Arguelles, M. C.; Russo, U. Diorganotin (IV) Derivatives of Salicylaldehydethiosemicarbazone. The Crystal Structure of Dimethyl- and Diphenyl- (Salicylaldehydethiosemicarbazonato)tin(IV). *Inorg. Chim. Acta* **1994**, *216*, 169 (b) Casas, J. S.; Castiñeiras, A.; Sánchez, A.; Sordo, J.; Vázquez-López, A.; Rodríguez-Arguelles, M. C.; Russo, U. Synthesis and Spectroscopic Propierties of Diorganotin(IV) Derivatives of 2,6-Diacetylpyridine Bis(thiosemicarbazone). Crystal Structure of Diphenyl{2,6-diacetylpyridine Bis(thiosemicarbazonato)}tin(IV) Bis(dimethylformamide) solvate. *Ibid.* **1994**, *221*, 61. (c) Mohan, M.; Sharma, P.; Kumar, M.; Jha, N. K. Metal Complexes of 2,6-Diacetylpyridine Bis(thiosemicarbazone): Their Preparation, Characterization and Antitumour Activity. *Ibid.* **1986**, *125*, 9.

(13) Chakladar, S.; Paul, P.; Venkatsubramanian, K.; Nag, K. Synthesis and Reactions of Cyclopalladated Compounds Derived from *N*,*N*′-Dialkylbenzene-1,3-dicarbaldimines [Alkyl = Ethyl (H$_2$L^1), Butyl or Octyl] and *N*,*N*′-Dibenzyl-benzene-1,3-dicarbaldimine. Crystal Structure of [Pd$_2$L^1(py)$_4$][ClO$_4$]$_2$. *J. Chem. Soc., Dalton Trans.* **1991**, 2669.

(14) Gutierrez, M. A.; Newkome, G. R.; Selbin, J. Cyclometalation Palladium 2-Arylpyridine Complexes. *J. Organomet. Chem.* **1980**, *202*, 341.

(15) Albert, J.; Ceder, R. M.; Gómez, M.; Granell, J.; Sales, J. Cyclopalladation of N-Mesitylbenzilidenamines. Aromatic versus aliphatic C.-H Activation. *Organometallics* **1992**, *11*, 1536.

(16) Thimmaiah, K. N.; Chandrappa, G. T.; Rangeswany; Jayarama. Structural Studies of Biologically active Complexes of Zinc(II) Cadmium(II), Mercury(II) and Copper(II) with *p*-Anisaldehyde Thiosemicarbazone. *Polyhedron* **1984**, *3*, 1237.

(17) Alley, M. C.; Scudiero, D. A.; Monks, A.; Huresey, M. L.; Czerwinski, M. J.; Fine, D. L.; Abbott, B. J.; Mayo, J. G.; Shoemaker, R. H.; Boyd, M. R. Feasibility of Drug Screening with Panels of Human-tumor Cell-lines Using a Microculture Tetrazolium Assay. *Cancer Res.* **1988**, *48*, 589.

(18) Sherman, S. E.; Lippard, S. J. Structural Aspects of Platinum Anticancer Drug-interactions with DNA. *Chem. Rev.* **1987**, *87*, 1153.
(19) Johnson, A.; Qu, Y.; Houten, B. V.; Farrell, N. *β*-Z DNA Conformational-changes Induced by a Family of Dinuclear Bis-(platinum) Complexes *Nucl. Acids Res.* **1992**, *20*, 1697.
(20) Roberts, J. R.; Houten, B. V.; Qu, Y.; Farrell, N. O. Interaction of Novel Bis(platinum) Complexes with DNA. *Nucl. Acids Res.* **1989**, *17*, 9719.
(21) Bax, A.; Morris, G. A. An Improved Method for Heteronuclear Chemical-shift Correlation by 2-Dimensional NMR. *J. Magn. Reson.* **1981**, *42*, 501.
(22) Sah, P. P. T.; Daniels, T. C. Thiosemicarbazide as a Reagent for the Identification of Aldehydes, Ketones and Quinones. *Recl. Trav. Chim. Pays-Bas* **1950**, *69*, 1545.
(23) Walker, N.; Stuart, D. An Empirical Method for Correcting Diffractometer Data for Absorption Effects. *Acta Crystallogr.* **1983**, A39, 158.
(24) *International Tables for X-ray Crystallography*; Kynoch Press: Birmingham, 1974; Vol. IV.
(25) Beurskens, P. T.; Admiraal, G.; Beurskens, G.; Bosman, W. P.; García-Granda, S.; Gould, R. O.; Smith J. M. M.; Smykalla, C. *The DIRDIF Program System*; Technical Report of the Crystallography Laboratory, Tournooiveld 6525 ED, Nijmegen, The Netherlands, 1992.
(26) Stewart, J. M.; Machin, P. A.; Dickinson, C. W.; Ammon, H. L.; Heck, H.; Flack, H. *The X-RAY 76 System of Crystallographic Program*; Computer Science Center, University of Maryland: College Park, Maryland, 1976.
(27) Martínez-Ripoll M.; Cano, F. H. *Programa PESOS*; Instituto Rocasolano, CSIC, Madrid, Spain, 1975.
(28) Spek A. L. PLATON, An Integrated Tool for the Analysis of the Results of a Single-Crystal Structure Determination. *Acta Crystallogr.* **1990**, A46, C34.
(29) Sheldrick, G. M. Phase Annealing in SHELX-90 Direct Methods for Larger Structures. *Acta Crystallogr.* **1990**, A46, 467.
(30) Sheldrick, G. M. *SHELX-96, Program for the refinement of crystal structure*; University of Göttingen: Göttingen, Germany, 1996.

JM970520D